p-ISSN 2089 – 0133 e-ISSN 2477-6416
URL: https://jurnal.uns.ac.id/ijap/article/view/71160

DOI: https://doi.org/10.13057/ijap.v15i1.71160

THE COMBINED BORIS-CYCLOTRONIC INTEGRATOR FOR AXIALLY SYMMETRIC PENNING ION SOURCE SIMULATION

Ahsani Hafizhu Shali*, Muhamad Rangga Del Piero
Research Center for Accelerator Technology, National Research and Innovation Agency (BRIN), Indonesia
*ahsani.hafizhu.shali@brin.go.id

Received 01-02-2023, Revised 21-03-2024, Accepted 28-02-2025,
Available Online 01-04-2025, Published Regularly April 2025

ABSTRACT

An investigation of the use of combined boris-cyclotronic particle integrator scheme for 2D axially symmetric Penning ion source simulation program has been performed. The particle-in-cell based simulation program was intended to be used for Penning ion source optimization. The combination was done by using cyclotronic integrator in cylindrical coordinates while ions were integrated using Boris algorithm (Boris-Cyclotronic scheme). The investigation was centered around the claim that cyclotronic integrator is not limited by gyration period constraints, unlike Boris algorithm. As a benchmark, this scheme is compared against the standard approach in which both species are integrated using the Boris algorithm (All-Boris scheme). The plasma sustainability result shows that for regions where time step width is smaller than the gyration period, Boris-Cyclotronic algorithm is indistinguishable from All-Boris algorithm. For time step width comparable to gyration period, there is an increase in electron production in Boris-Cyclotronic algorithm while All-Boris algorithm remains the same. Single-particle tests show that although the Boris integrator produces noisy trajectories, it maintains a bounded energy error and a consistent average path. In contrast, the cyclotronic integrator produces smoother trajectories but introduces significant oscillatory energy gain, which leads to artificial ionization and exaggerated electron production. These findings indicate that despite its less accurate individual trajectories, the All-Boris scheme provides more physically consistent results for Penning ion source simulation than the Boris–Cyclotronic scheme.

Keywords: Penning ion source; particle-in-cell; cyclotronic integrator.

Cite this as: Shali, A. H., & Piero, M. R. D. 2025. The Combined Boris-Cyclotronic Integrator for Axially Symmetric Penning Ion Source Simulation. *IJAP: Indonesian Journal of Applied Physics, 15*(1), 17-32. doi: https://doi.org/10.13057/ijap.v15i1.71160

INTRODUCTION

The Research Center for Accelerator Technology is currently developing a compact cyclotron for medical use[1-2]. The cyclotron accelerates negative hydrogen ions with a maximum energy of 13 MeV to be bombarded to enriched water, resulting in Fluorine-18 isotope production. The isotope is used for cancer diagnostic by means of *Positron Emission Tomography* (PET) method[3]. A Penning ion source is placed inside the central region of the cyclotron to provide a steady stream of negative hydrogen ions to be accelerated by the accelerating structure.

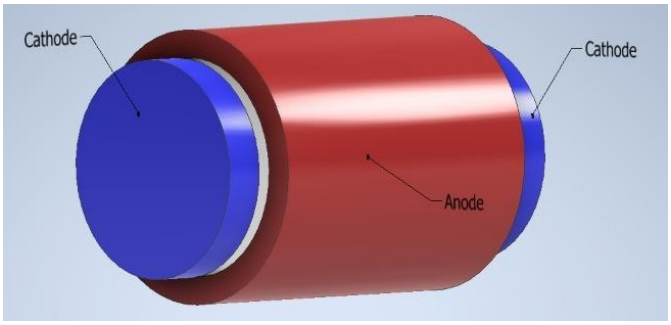

Figure 1. A simple Penning ion source model

The standard Penning ion source is cylindrically shaped with its top and bottom acting as cathodes, while the sheath is electrically grounded[4-5] as shown in Figure 1. A steady flow of low-pressure gas (which in this case is hydrogen gas) is injected to the chamber. Electrical discharge from the application of electric potential will generate plasma inside the ionization chamber. Additionally, a static axial magnetic field is applied to the ionization chamber to confine electrons inside the chamber, which will increase the probability of close-range interactions, such as ionization, before electrons finally hit the boundary of the domain[5]. The increase of close-range interactions will eventually increase the degree of the ionization of the plasma, which means that the amount of produced negative hydrogen ions will increase. The rate of production of negative hydrogen ions will depend on the choice of parameters such as the strength of magnetic field, cathode potential, ionization chamber size, gas flow, etc.

The optimized rate of negative hydrogen ion production can be achieved by varying the parameters mentioned previously. However, blindly varying the parameters to get the optimal setup is not efficient, since some of the parameters such as the dimension of the ion source cannot be modified easily. Unfortunately, analytical calculation to predict the rate of production of negative hydrogen ions given some initial parameters does not seem to be possible due to the complexity of the problem. Thus, numerical simulation is usually the preferred method to estimate the outcome of plasma experiments[6].

There are several numerical schemes that can be used to simulate plasmas, depending on the scale of the plasma and the needed accuracy of the simulation. If the scale of the plasma is large (such as plasmas on stars), numerical simulation based on fluid dynamics is more suitable. For smaller devices such as a glow discharge ion source where detailed processes are required, simulation based on kinetic scheme, where particles are simulated instead, is a better option[7]. The fundamentals of plasma simulation based on kinetic scheme is simple: given a distribution of charged particles inside the domain, the particle-to-particle interactions along with the influence of external electric and magnetic fields are calculated. After that, the equations of motion of the particles are numerically solved for a given small time step width. The process is then repeated so that the macroscopic evolution of the plasma is obtained. Note that schemes to simulate short range interactions such as elastic collisions, excitations, and ionization can be placed after each integration of the equation of motions[8]. However, due to the limitation of computers, it is not possible to calculate the interaction of each particle (i.e., by coulomb force) since a typical plasma device contains a gigantic amount of charged particles. Instead, electric forces are calculated using Poisson equation by first translating the spatial distribution of charged particles into the distribution of charge density in a specific mesh that was initially defined[9]. Accordingly, the scheme is called the *particle-in-cell* scheme. The number of particles needed to run the simulation can also be

reduced by particle weighting, i.e. each simulated particle (called a macroparticle) represents a lot of real physical particles.

One part of particle-in-cell scheme is the equations of motion integrator/solver, which predict the final position and velocity of a particle given a small-time step width and field distribution[10]. Currently the most popular solver to solve the motion of charged particles under the influence of magnetic field is the Boris algorithm[11] because of the second order accuracy, relatively low computational cost, and time symmetry. However, Boris algorithm suffers from the need of smaller time steps width relative to the gyration period[6] thus might be too costly for some cases. For a more specific case where the magnetic field is homogeneous, cyclotronic integrator[12] offers better accuracy without requiring smaller time step width. Coincidentally, the magnetic field inside the ionization chamber of a Penning ion source inside DECY-13 cyclotron is homogeneous, which means that the cyclotronic integrator is more suitable to be used. Further, due to the axial symmetry of the ion source, the domain can be simplified into a two-dimensional axially symmetric (r-z) domain, which greatly decreases the computational cost[13]. Hence, the integration of the equation of motion needs to be done in cylindrical coordinates.

In addition, the property of bounded numerical error exhibited by Boris algorithm in cartesian coordinates[11] might not be retained when the algorithm is applied in cylindrical coordinates. In contrast, cyclotronic integrator, even when applied in cylindrical coordinates, is symplectic. It means that it can be guaranteed that the phase space volume of the system is (or almost) conserved[14]. Effectively, the error of cyclotronic integrator is bounded[15]. Thus, for simulations requiring long term accuracy, integrators that preserve phase space volume are preferred, such as the cyclotronic integrator.

In this paper, a plasma simulation program written in C++ for Penning ion source optimization based on Particle-in-cell algorithm is proposed. The program used a combination of cyclotronic integrator in cylindrical coordinate and Boris algorithm in cylindrical coordinate. The cyclotronic integrator is used due to its long-term accuracy and a more relaxed requirement of time step width, while the Boris algorithm is used for particles that move slowly and close to the z-axis. Effectively, electrons are pushed using the cyclotronic integrator, while ions are pushed using Boris algorithm (Boris-Cyclotronic schemes). The program is then compared with a particle-in-cell program purely using Boris algorithm in cylindrical coordinates (All-Boris schemes).

Previously, most simulation of negative hydrogen Penning ion source was not done in self-consistent manner, where ions and electrons production rate was determined by some initial parameters, and not the energy distribution of the constituents of the plasma itself [16–18]. Some authors ignored plasma dynamics when simulating the performance of a Penning ion source[4]. One of the published self-consistent plasma simulation of Penning ion source has been done[13], but particles are wholly integrated using Boris algorithm. However, Boris algorithm is problematic if the time step width is comparable to gyration period[12]. This research is intended to investigate the possibility of the use of cyclotronic integrator for electron component of Penning ion source plasmas with large time step width, due to the fact that cyclotronic integrator still retain its accuracy for step width comparable to the gyration period[12].

To analyze the numerical errors for either of the schemes, several simulation results are going to be compared. The first one is the spatial distribution of particles to see if both schemes predict similar distribution macroscopically, with two different time step width.

Stark difference of particle spatial distribution between algorithms means that there is something wrong with the simulation code. The second one is the energy distribution of particles, especially electrons. Penning ion source require a particular energy distribution of electron so that the plasma is sustained while at the same time negative hydrogen ions production is maintained[13]. The energy distribution will depend on the individual kinetic energy of each particle, which in turn depends on the velocity of each particle. Therefore, errors (especially added up errors at the later stage of simulation) will greatly affect the energy distribution of electrons.

METHOD

General Scheme

Charged particles inside the domain are simulated using particle-in-cell monte-carlo collision. The schematics of particle-in-cell monte-carlo collision algorithm is shown in Figure 2**.** Due to the symmetry of the domain, the simulation is done in two axially symmetric spatial dimensions with structured rectangular meshes to reduce computational cost. The velocity vector of a simulated particle is still three-dimensional, which is often called the 2d3v scheme.

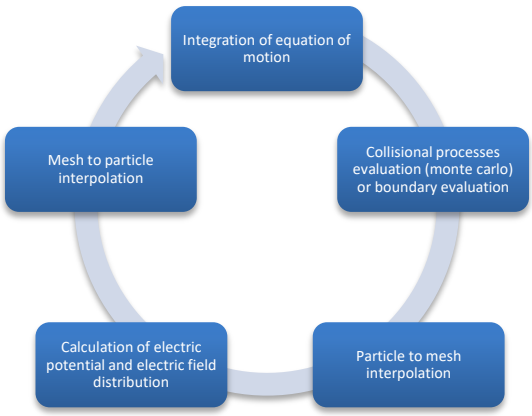

Figure 2. The flow schematics of particle-in-cell algorithm

Only electrons, H+, H2+, and H- are simulated, highly ionized particles are assumed to be rare, while neutral gas (H2 and H) are considered as background fluid with uniform density. Due to the slowness of neutral gas (compared to electrons and ions), it is assumed that the velocities of neutral gas particles are equal to zero. Another assumption is that the plasma inside a Penning ion source is lowly ionized, which means that neutral particles are much more numerous compared to charged particles[13]. Based on those assumptions, interactions between charged particles and neutral gas can be simulated using null-collision monte carlo collision[19].

Particle-to-mesh and mesh-to-particle interpolation are both implemented using first order interpolation[20]. For low-temperature plasma, it is safe to assume that most particles move relatively slowly (in eV region), which means that induced self-magnetic field can be ignored. In addition, electric potential from the external source is not varying with respect to time, thus static electric field assumption $\vec{E} = -\nabla V$ can be used. Electric potential from Poisson equation with a combination of Dirichlet and Neumann boundary conditions is solved with the standard Gauss-Seidel method in cylindrical coordinates[20]. At the $r = 0$ boundary, the radial electric field is assumed to be equal to zero, while Gauss' law can be

used to evaluate the potential at the boundary. The domain is connected to external circuit as shown below[13] with source voltage fixed.

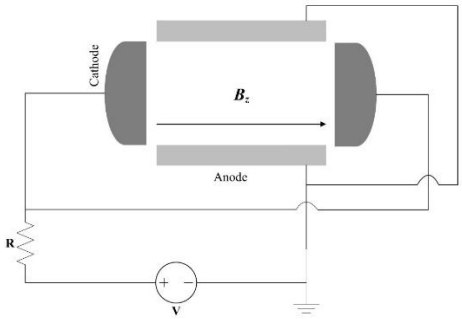

Figure 3. Simple external circuit model for Penning ion source

The equations of motion of charged particles are integrated numerically using a combination of non-relativistic Boris algorithm in cylindrical coordinates[6] and cyclotronic integrators in cylindrical coordinates[21]. Cyclotronic integrator has a better long-term accuracy compared to Boris algorithm due to its phase-space preserving property[12]. Conversely, Boris algorithm is better suited for particles that move close to the z-axis, since at lower radii, the error of the cyclotronic integrator in cylindrical coordinates becomes much larger due to $1/r$ dependency. Therefore, the cyclotronic integrator is suitable for electrons due to the fact that most electrons are expected to be pushed away from the z-axis[13]. Positive ions are pulled toward the z-axis, some have a really small radial position, which makes Boris algorithm more suitable. In addition, ions gyrate much more slowly compared to electrons under the same magnetic field distribution[20], thus the error due to large time step width relative to gyration frequency is minimal.

The result with the combined solver above will be compared with an identical particle-in-cell simulation wholly integrated with Boris algorithm. Energy distribution of electrons in both cases are compared with each other. The number of particles for each case is also compared, to see whether changing the solver causes an observable difference or not.

Particle Mover Algorithm

The first particle mover to consider is the non-relativistic Boris algorithm in cylindrical coordinates. The algorithm is done by first discretizing Lorentz equations as follows[22]

$$m\frac{d\vec{v}}{dt} = q\vec{E} + q\vec{v} \times \vec{B} + \vec{F}_{in} \tag{1}$$

where $\vec{F}_{in}$ stands for inertial forces and $\vec{v}$ is the average of velocity of $n + 0.5$ and $n - 0.5$ steps (velocities are evaluated at half integer steps, while positions are evaluated at integer steps). The components of inertial forces are $\left(v_\theta^2/r, -v_\theta v_r/r, 0\right)$ which are the centripetal and coriolis forces. It is possible to do calculations without those inertial forces by rotating the coordinate instead[21]. For simplicity, let's say that the magnetic field is directed along the z-axis, which means that the particle will gyrate on the x-y plane. After an iteration, the particle would be located at x' and y' outside the initial r-z plane. The plane is then rotated with an angle α so that the particle is located on the r-z plane again. The angle α is defined as

$$cos\,\alpha = \frac{x'}{r} \qquad sin\,\alpha = \frac{y'}{r} \qquad r = \sqrt{x'^2 + y'^2} \tag{2}$$

Note that the velocities also need to be rotated back to accommodate coordinate transformation. If at the final position the particle is at the z-axis (thus $r = 0$) it can be assumed that $sin\,\alpha = 0$ and $cos\,\alpha = 1$, which means that at that point the velocity is entirely radial. Radial position error can be avoided at the cost of error from sine, cosine, and square root error.

Unlike Boris algorithm, cyclotronic algorithm is a symplectic integrator, designed only for charged particles moving under the influence of homogenous magnetic field[12]. The integrator maps the flow of the position and momentum of a particle using Poisson bracket, $\frac{dz}{dt} = \{z, H\}$ where $z = (q, p)$ is a collection of position and momentum of the particle and H is the Hamiltonian of the system. The bracket is usually written as an operator $\{z, H\} = D_H z$, which means that the flow of z can be written as $z(\tau) = exp(\tau D_H)\, z(0)$[12] which maps $z(0)$ into $z(\tau)$. Note that the operator needs to be calculated analytically using Poisson bracket. If it turns out that it is not possible to analytically calculate the operator, it is possible to use splitting algorithm to separate the Hamiltonian into several parts (most of the time, two parts)[23]. For cyclotronic integrator in cylindrical coordinates the choice of splitting is as follows

$$H = H_D + H_K \tag{4}$$

$$H_D = \frac{p_z^2}{2m} + \frac{p_r^2}{2m} + \frac{1}{2m}\left(\frac{p_\varphi}{r} - QA_\varphi\right)^2 \tag{5}$$

$$H_K = -Q\phi \tag{6}$$

which is used for cases where the magnetic field is static and axially homogeneous, while the electric field is slowly varying[12]. The D and K subscript stand for drift and kick respectively. The second order approximation for $exp(\tau D_H) = exp(\tau D_D + \tau D_K)$ is given by $exp(\tau D_H) = exp(0.5\tau D_D)\, exp(\tau D_K)\, exp(0.5\tau D_D) + O(\tau^3)$ which can be done using Baker-Campbell-Haussdorff formula [12]. The operator for both drift and kick part are actually calculated using the conservation equations (conservation of energy and angular momenta, which is given by[21]

1. Kick part $exp(\tau D_K)$

$$v_r^* = v_r^0 + \frac{q\Delta t E_r}{m} \qquad r^* = r^0 \tag{7}$$

$$v_\varphi^* = v_\varphi^0 + \frac{q\Delta t E_\varphi}{m} \qquad \varphi^* = \varphi^0 \tag{8}$$

$$v_z^* = v_z^0 + \frac{q\Delta t E_z}{m} \qquad z^* = z^0 \tag{9}$$

2. Drift part $exp(\tau D_D)$

$$r^* = \left[(r^0)^2 cos(\omega\Delta t) + \frac{4E^0 + 2\omega P_\varphi^0}{\omega^2}(1 - \cos(\omega\Delta t)) + \frac{2r^0 v_r^0}{\omega}\sin(\omega\Delta t)\right]^{\frac{1}{2}} \tag{10}$$

$$\varphi^* = \varphi^0 - \frac{\omega\Delta t}{2} + \frac{2P_\varphi^0\omega}{\alpha^0}\left[\tanh^{-1}\left(\frac{2r^0 v_r^0 \omega}{\alpha^0}\right) - C^0\right] \tag{11}$$

$$z^* = z^0 + v_z^0\Delta t \tag{12}$$

$$v_r^* = \frac{1}{r^*}\left[r^0 v_r^0 \cos(\omega\Delta t) - \frac{\omega(r^0)^2}{2}\sin(\omega\Delta t) + \frac{2E^0 + \omega P_\varphi^0}{\omega}\sin(\omega\Delta t)\right] \tag{13}$$

$$v_\varphi^* = \frac{P_\varphi^0}{r^*} - \frac{\omega r^*}{2} \tag{14}$$

$$v_z^* = v_z^0 \tag{15}$$

Several parameters written above are defined as follows,

$$C^0 = \tanh^{-1}\left[2\frac{2r^0 v_r^0 \omega}{\alpha^0} + 8\frac{8E^0 + 4\omega P_\varphi^0 - \omega^2 (r^0)^2}{\alpha^0}\tan\left(\frac{\omega \Delta t}{2}\right)\right] \quad (16)$$

$$\alpha^0 = \omega r^0 \left[4(v_r^0)^2 - 8E^0 - 4\omega P_\varphi^0 + (\omega\, r^0)^2\right]^{\frac{1}{2}} \quad (17)$$

$$E^0 = \frac{(v_r^0)^2 + (v_\varphi^0)^2}{2} \quad (18)$$

$$P_\varphi^0 = r^0 v_\varphi^0 + \frac{\omega (r^0)^2}{2} \quad (19)$$

Where the asterisks indicate the value of positions or velocities after the operator is applied, and the superscript zeros before it.

Simulation Setup

The domain for the simulation for both Boris-Cyclotronic scheme and All-Boris scheme is shown in Figure 4 below.

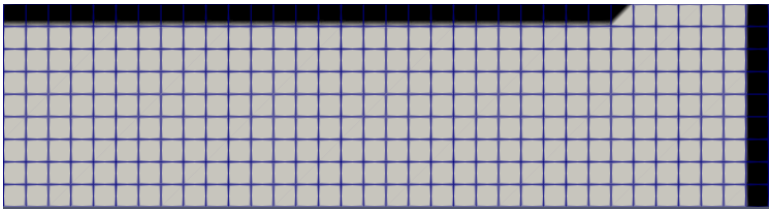

Figure 4. The domain of simulation

The domain is an axially symmetric $r - z$ plane mirrored at $z = 0$ plane, to decrease computing time without losing accuracy. The cathode is connected to an external circuit following[13] as shown in Figure 3,

Table 1 shows the parameters used for the simulation.

Table 1. Simulation parameters

No.	Parameter	Symbol	Value
1.	Axial length (one half)	L_z	17.5 mm
2.	Radial length	L_R	5 mm
3.	Neutral gas pressure	P	0.005Pa
4.	Gas Temperature	T_N	300 K
5.	Atom to molecule number density ratio	n_H/n_{H_2}	0.2
6.	Density ratio of the vibrationally excited state with $\nu = 4$	$n_{H_2(\nu=4)}/N_{H_2}$	0.1
7.	Axial magnetic field	B_z	1.1 T
8.	Secondary electron emission coefficient from cathodes	γ	0.1
9.	Cathode electric potential	V_c	-1300 V
10.	Anode electric potential	V_a	0 V
11.	Mesh size	$\Delta r, \Delta z$	0.5 mm
12.	Time step width	Δt	30 ps
13.	Iteration number	N_{iter}	1.5×10^6
14.	Macroparticle weight	w_{sp}	4×10^5
15.	External resistor	R	1kΩ

The general formulation for plasma-external circuit interaction can be found in [24]. When an ion hits the cathode, there is a $\gamma \times 100\%$ chance that a secondary electron is ejected from

the cathode, where γ is the secondary emission coefficient. The processes included for null-collision monte-carlo collision are shown in Table 2.

Table 2. Close range processes included in the simulation.

No.	Reactions	References
1.	$e + H \rightarrow e + H$ (elastic)	[25]
2.	$e + H \rightarrow 2e + H^+$	[25]
3.	$e + H_2 \rightarrow e + H_2$ (elastic)	[26]
4.	$e + H_2 \rightarrow 2e + H_2^+$	[26]
5.	$e + H_2 \rightarrow 2e + H + H^+$	[26]
6.	$e + H_2 \rightarrow H + H^-$ (11 subprocesses)	[26]

Not all processes are included in this simulation since the main point of this research is to compare the performance between two schemes of integration. Processes such as excitation of electronic states will generally lower the energy distribution of simulated particles. Thus, relative energy distribution between two integration schemes will not be that different. In addition, since the plasma inside the domain is not highly ionized, then most of the constituents of the plasma are neutral particles (about 100 times more numerous[13]). Which means that compared to charged-neutral close-range interactions, charged-charged close-range interactions are very rare. Therefore, omitting close range processes between charged particles would not cause an observable difference in the outcome of the simulation.

Initial electron macroparticles are randomly injected with a homogenous spatial distribution inside the domain with initial kinetic energy of 3 eV. The initial velocity is randomly distributed and follows Maxwellian distribution. The positive ions are injected with similar initial spatial distribution so that the plasma is initially neutral. Because of the sluggishness of positive ions compared to electrons, the ions are initially sampled with zero initial velocity.

The axial magnetic field is chosen to be quite high, specifically to match the working condition of Penning ion source inside a compact cyclotron. The specific value of 1.1 T of axial magnetic field and time step width of 30 ps are chosen to match the simulation condition of Penning ion source by Abadi et. al.[13]. The gas pressure is set to be very low, since higher pressure means that a lot of gas particles will seep into the vacuum chamber of the cyclotron. The test is replicated with smaller time step width of 10 ps,

The comparison is done by analyzing several results obtained using both schemes. The second one is the number of simulated macroparticles with respect to time. The simulation is designed to be self-consistent (particle injection is done using physical process, such as ionization or secondary electron emission, except for initial injection), which means that at some point the number of macroparticles is expected to have a steady value, indicating that the plasma is sustained inside the domain. The third one is the energy distribution of macroparticles at the initial and later stages of simulation. The energy distribution indicates how the plasma is heated using applied external voltage. The fourth one is single particle tracking simulation, to see how particle behaves, especially for larger time step width.

RESULTS AND DISCUSSION

The first comparison that needs to be made is the final spatial distribution of both schemes to check whether there is any significant difference between the two schemes. The following number density distribution of electron are calculated after 0.21 μs (or about 210000 iterations).

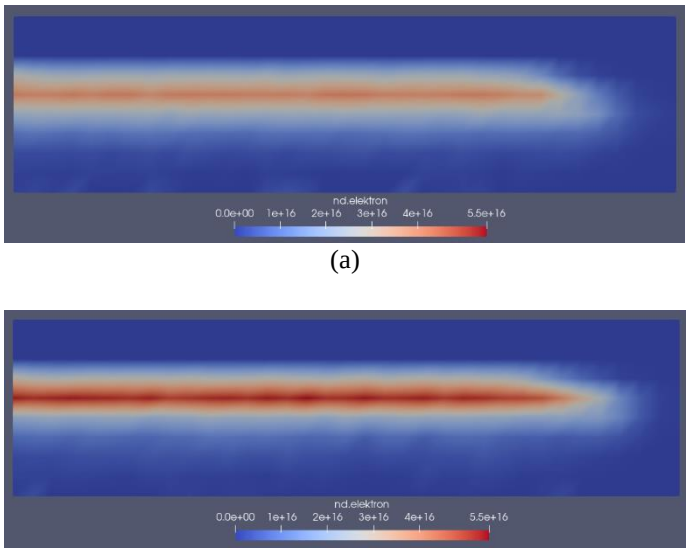

(a)

(b)

Figure 5. Electron spatial distribution after 210000 iterations with 30 ps width for (a) All-Boris scheme, (b) Boris-Cyclotronic scheme.

It can be seen from Figure 5 above that in general the spatial distribution of electrons for both cases are relatively the same. Since both schemes agree on the predicted spatial distribution, it can be said that numerically both algorithms are correct. However, it is evident that for All-Boris case, the electron density is visibly lower around the same region. Which means that at that point, the amount of simulated electron macroparticle for all-Boris algorithm is lower compared to Boris-Cyclotronic algorithm. Therefore, the evolution of the number of electrons macroparticles for both schemes needs to be investigated.

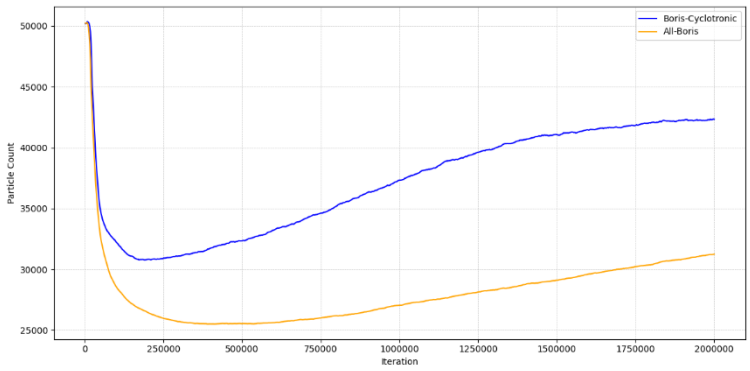

Figure 6. Electron macroparticle numbers as a function of iteration steps for Boris-Cyclotronic and All-Boris schemes.

The results for time evolution of macroparticles of Boris-Cyclotronic integrator and all Boris integrator are shown in Figure 6. Only the evolution of macroparticle number of electrons and negative hydrogen ion are shown here. The evolution of macroparticle number of

electrons indicate the sustainability of the plasma, with low electron counts means that plasma is not sustainable. In general, not all configuration of parameters will give a sustainable plasma (*e.g.*, too low pressure will reduce electron and ion production rate), a steady state is achieved when the production rate plasma constituents (such as electron) are equal to the rate of decrement of the constituent (such as when macroparticles crosses conductor boundaries).

As can be seen, the macroparticle number of electrons for Boris-Cyclotronic scheme is stable at about 42000 macroparticles after about 2000000 iteration steps. While for the All-Boris scheme, the number of electrons macroparticle is lower at about 31000 macroparticles. It can be inferred for All-Boris scheme that the rate of electron production is lower than electron production rate in Boris-Cyclotronic algorithm. Due to the similarity of spatial distribution of electrons between All-Boris and Boris-Cyclotronic schemes, it is reasonable to conclude that for both cases electron macroparticles are destroyed in similar manner (such as by hitting the anodes). The difference of electron macroparticle number thus comes from the difference in electron production rate. As can be seen from Table 1., electrons are produced from ionization processes (along with secondary electron emission). For this process to happen, electrons need to have an energy of 16 eV and 13.6 eV for molecular and atomic ionization respectively[25,26] which can be obtained by applying external electric potential. It is then reasonable to guess that electrons simulated using the All-Boris scheme has a lower average kinetic energy distribution compared to Boris-Cyclotronic scheme. Since the physical setup of the simulation is the same for both schemes, it means that there are some numerical errors in particle velocity, especially after a long period of iteration. To further investigate the error, the kinetic energy distribution for both schemes need to be compared. Figure 7 shows the energy distribution of electron for both schemes,

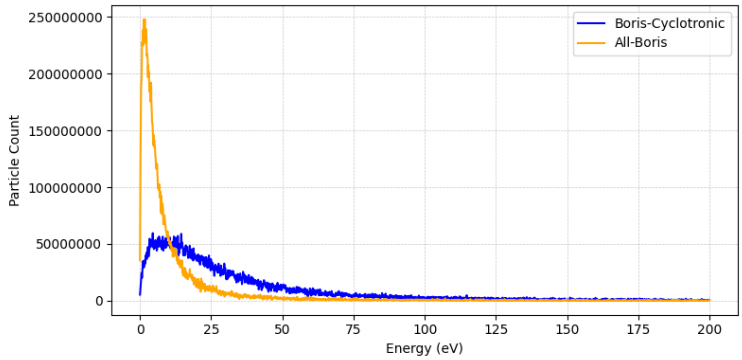

(a)

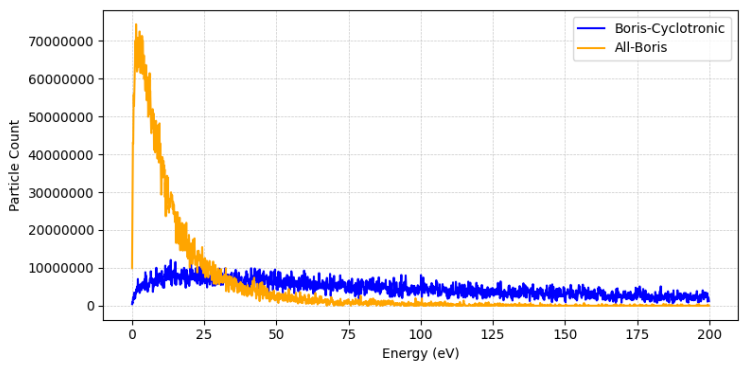

(b)

Figure 7. Electron energy distribution for Boris-Cyclotronic and All-Boris schemes after (a) 5000 iterations and (b) 210000 iterations.

It is evident that although initially the energy distribution of electrons for both cases are the same, most of electrons in the All-Boris scheme have a low energy (below 10 eV). This will inevitably hinder the electron production process from ionization, which is the main contributor for electron production. Compared to the All-Boris scheme, the energy distribution of Boris-Cyclotronic scheme is more spread out, there are just as much higher energy electrons as lower energy ones. This way the plasma can be sustained while at the same time, production of negative hydrogen ion is maintained since negative hydrogen ions are created by low energy electrons[13], as evident in Figure 8. However, as can be seen from equations (2), (9), and (15), the axial (z-directed) component updates are identical. Which means that the error should not come from axial component of particle velocities. To prove that assertion, the plot for energy distribution based on non-axial part (using $E_{\perp} = \frac{1}{2}m(v_r^2 + v_z^2)$) is given in Figure 9 below,

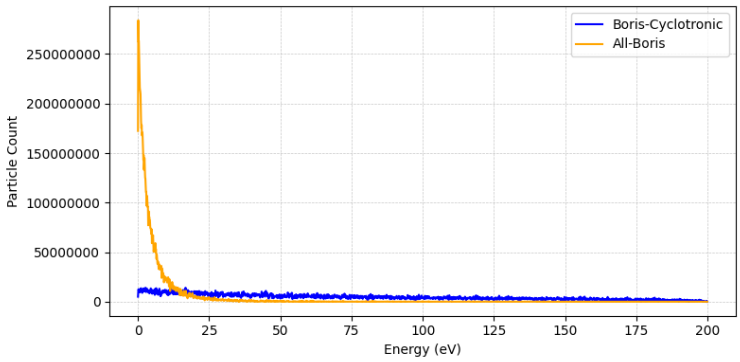

Figure 8. Non-axial energy distribution of electrons for Boris-Cyclotronic and All-Boris schemes after 210000 iterations.

It is clear that All-Boris scheme has significantly less particles with higher non-axial velocities compared to Boris-Cyclotronic scheme. This could mean either the electrons in All-Boris scheme experience numerical damping, or the electrons in Boris-Cyclotronic scheme experience numerical heating. As seen from Figure 8 the damping is significant to the reduction of the kinetic energy of the electron. This non-axial velocity damping (or heating) is likely coming from coordinate rotation shown in equation (2. However, both of the algorithms are time-reversible, which means that the heating or damping are likely bounded[11].

More accurate simulation can be done using smaller time step width. The exact same simulation is performed with a time step width of 10 ps, which is about a third of the gyration period. Theoretically, this time step width is still too big for Boris algorithm to be accurate. Figure 9 shows the spatial distribution of electron number density after 630000 iterations (equal to 210000 iterations for 30 ps time step width). It is evident that the distribution is almost identical between Boris-Cyclotronic and All-Boris scheme. Figure 10 shows the comparison of macroparticle number evolution for both of the scheme, which shows that the electron macroparticle number is with respect to time is essentially the same. The macroparticle number for both of them is around 25000, as shown in Figure 10, which is identical with the result of All-Boris algorithm for 30 ps time step width. This shows that for 30 ps case, the electron integrated using Cyclotronic algorithm experience numerical error related to its kinetic energy.

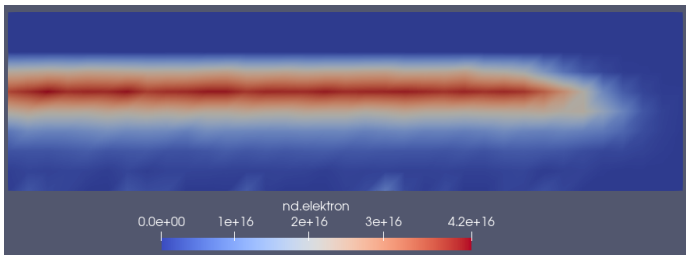

(a)

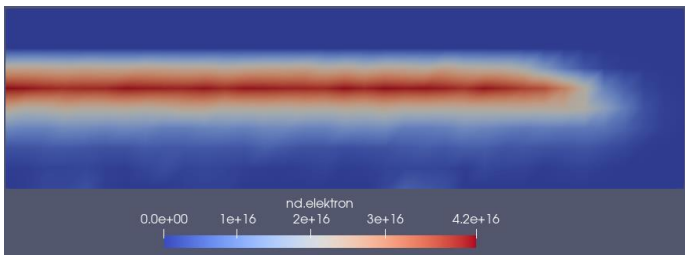

(b)

Figure 9. Electron spatial distribution after 630000 iterations with 10 ps time setp width for (a) All-Boris scheme, (b) Boris-Cyclotronic Scheme.

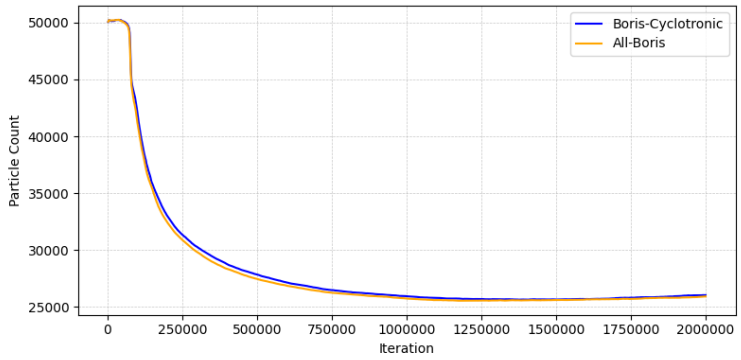

Figure 10. Electron macroparticle numbers as a function of iteration steps for Boris-Cyclotronic and All-Boris schemes, with dt = 10 ps.

Figure 11 shows the comparison kinetic energy distribution for Boris-Cyclotronic and All-Boris case for 10 ps time step width after 630000 iterations. It can be seen that the kinetic energy distribution difference that was apparent in previous case is not present here.

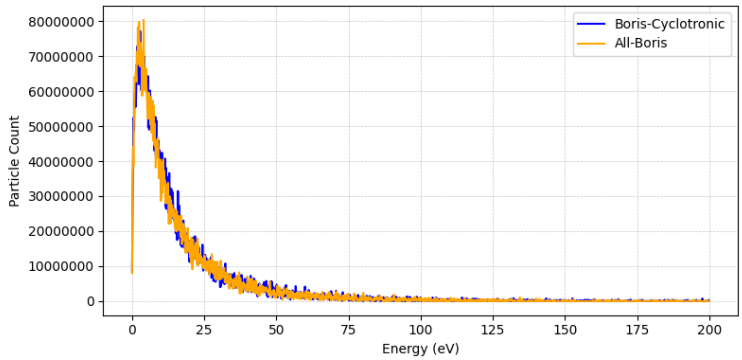

Figure 11. Electron energy distribution for Boris-Cyclotronic and All-Boris schemes after 630000 iterations with dt = 10 ps.

To investigate further, plot of single particle trajectories between two schemes are compared, with the same set up parameters as the previous simulation (with time step width of 30 ps). A single electron is sampled with an initial position of $\vec{x} = (0.0145,0.003)$ m and $\vec{v} = (0,0,2297054)$ m/s where the velocity is related to electron kinetic energy of 30 eV. The trajectories for earlier iterations (step 0 to 100) are compared to the trajectories at a relatively later times (step 999900 to 1000000) to show the possible presence of numerical error accumulation.

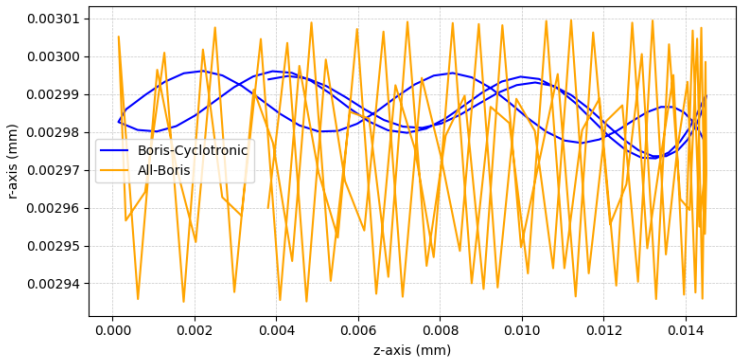

(a)

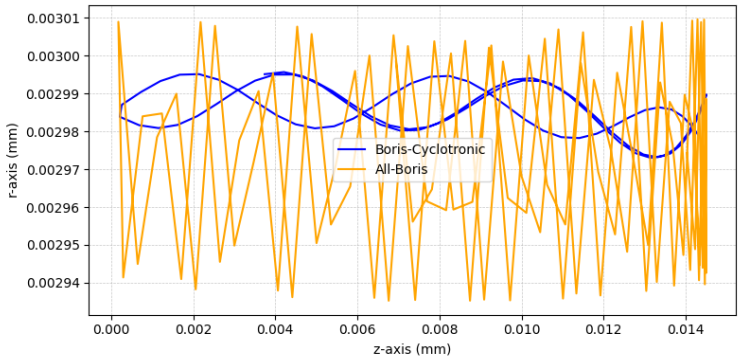

(b)

Figure 12. Single electron trajectories for Boris-Cyclotronic and All-Boris schemes at (a) earlier iterations and (b) later iterations.

Figure 12 shows that the error for both schemes are bounded, as evident by particles having similar average radial position after many iterations. The gyration radius is also the same for both schemes for earlier and later iterations. Electrons integrated using All-Boris scheme has an erratic movement stemming from the fact that Boris algorithm cannot accurately integrate particle position if time step width is too large. Such problem is not faced by cyclotronic algorithm, since the electron movement is rather smooth. Still, the fact that in macroscopic scale All-Boris scheme is more accurate than Boris-Cyclotronic scheme (indicated by electron macroparticle number evolution), means that electrons integrated using Cyclotronic integrator experience some unphysical kinetic energy heating. Figure 13 shows the comparison between electron non-axial kinetic energy for All-Boris scheme and Boris-Cyclotronic scheme. It can be seen that particles integrated using Boris-Cyclotronic scheme experience some non-negligible heating, while All-Boris scheme did not.

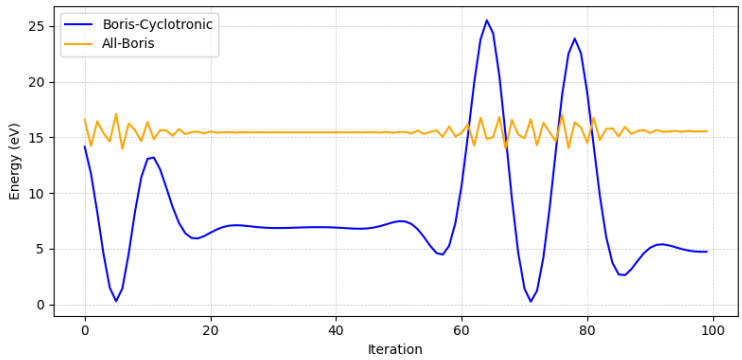

(a)

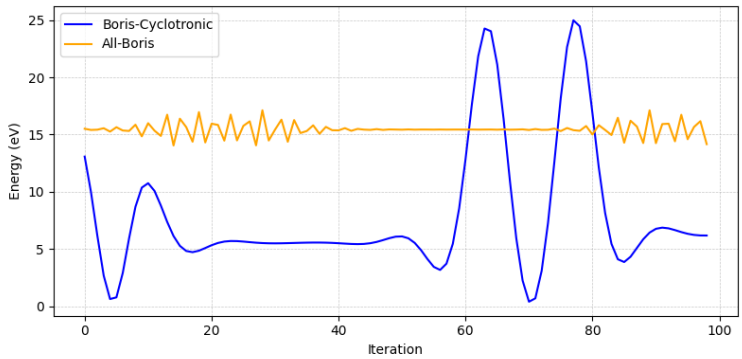

(b)

Figure 13. Single electron non-axial kinetic energy for Boris-Cyclotronic and All-Boris schemes at (a) earlier iterations and (b) later iterations.

Based on results explained above, it can be inferred that the claimed advantage of bigger time step width tolerance of cyclotronic algorithm compared to Boris algorithm does not really matter for Penning ion source simulation. The erratic movement of individual electrons integrated using Boris algorithm does not accumulate into visible error on macroscopic scale, as the rate of electron production via ionization is not greatly affected. It is also evident that for time step width comparable to gyration period, cyclotronic integrator experience oscillatory kinetic energy heating which can erroneously increase electron production, while the Boris algorithm remains bounded as before. Cyclotronic algorithm should be more suitable for cases where individual position of electrons needs to be determined accurately each step, such as for particle tracking for beam dynamics simulation. Therefore, for Penning ion source simulation, in which individual particle accurate position does not matter, Boris algorithm is still a more suitable option.

CONCLUSION

The proposed combined Cyclotronic-Boris scheme implemented to a 2D axially symmetric Penning ion source simulation code has been analyzed. The scheme has also been compared with a similar code based on All-Boris scheme. The result shows that despite higher microscopic accuracy of Boris-Cyclotronic shceme, macroscopic result suffers some error from unphysical increase of electron production, stemming from oscillatory kinetic energy heating of electron. All-Boris scheme did not suffer from such error due to the absence of artificial kinetic energy heating, although the movement of each individual electron is not accurate. This finding shows that even though cyclotronic algorithm is more accurate for

each individual particle compared to Boris algorithm, especially for larger time step width, it does not make it better than Boris algorithm for Penning ion source simulation. Boris algorithm is still a preferable choice for larger time step width.

ACKNOWLEDGMENTS

This research was supported by the Research Center for Accelerator Technology, National Research and Innovation Agency. We specifically thank Mr. Silakhuddin for the useful insight about the design and the working principle of Penning ion source. We also thank the head of our research group, Dr. Taufik for his encouragement on this topic of research.

REFERENCES

1 Taufik, Hermanto, A., Anggraita, P., & Santosa, S. 2014. Determination of magnet specification of 13 MeV proton cyclotron based on opera 3D. *Atom Indonesia*, *40*(2), 69–75.

2 Silakhuddin, S., Darmawan, R. S., Suharni, S., Permana, F. S., Wibowo, K., Saminto, S., & Atmono, T. 2018. Ion beam preliminary testing of DECY-13 cyclotron at the central region using dc extraction voltage. *IOP Conference Series: Materials Science and Engineering*, *432*(1).

3 Jacobson, O., Kiesewetter, D. O., & Chen, X. 2015. Fluorine-18 radiochemistry, labeling strategies and synthetic routes. *Bioconjugate Chemistry*, *26*(1), 1–18.

4 Yeon, Y. H., Ghergherehchi, M., Mu, X., Gad, K. M. M., & Chai, J. S. 2014. Development and discharge characteristics of negative hydrogen ion source for the SKKUCY-9 cyclotron. *Nuclear Instruments and Methods in Physics Research, Section A: Accelerators, Spectrometers, Detectors and Associated Equipment*, *763*, 510–516.

5 Bacal, M., & Wada, M. 2015. Negative hydrogen ion production mechanisms. *Applied Physics Reviews*, *2*(2).

6 Birdsall, C. K. 1991. Particle-in-Cell Charged-Particle Simulations, Plus Monte Carlo Collisions With Neutral Atoms, PIC-MCC. *IEEE Transactions on Plasma Science*, *19*(2), 65–85.

7 Ripperda, B., Bacchini, F., Teunissen, J., Xia, C., Porth, O., Sironi, L., Lapenta, G., & Keppens, R. 2018. A Comprehensive Comparison of Relativistic Particle Integrators. *The Astrophysical Journal Supplement Series*, *235*(1), 21.

8 Juhasz, Z., Ďurian, J., Derzsi, A., Matejčík, Š., Donkó, Z., & Hartmann, P. 2021. Efficient GPU implementation of the Particle-in-Cell/Monte-Carlo collisions method for 1D simulation of low-pressure capacitively coupled plasmas. *Computer Physics Communications*, *263*, 107913.

9 Langdon, A. B. 2014. Evolution of particle-in-cell plasma simulation. *IEEE Transactions on Plasma Science*, *42*(5), 1317–1320.

10 Zenitani, S., & Kato, T. N. 2020. Multiple Boris integrators for particle-in-cell simulation. *Computer Physics Communications*, *247*(xxxx), 106954.

11 Qin, H., Zhang, S., Xiao, J., Liu, J., Sun, Y., & Tang, W. M. 2013. Why is Boris algorithm so good? *Physics of Plasmas*, *20*(8), 084503.

12 Patacchini, L., & Hutchinson, I. H. 2009. Explicit time-reversible orbit integration in Particle In Cell codes with static homogeneous magnetic field. *Journal of Computational Physics*, *228*(7), 2604–2615.

13 Rafieian Najaf Abadi, M., Mahjour-Shafiei, M., & Yarmohammadi Satri, M. 2018. Simulation and optimization of a negative hydrogen Penning ion source. *Physics of Plasmas*, *25*(12).

14 Tao, M. 2016. Explicit high-order symplectic integrators for charged particles in general electromagnetic fields. *Journal of Computational Physics*, *327*(September), 245–251.

15 He, Y., Sun, Y., Liu, J., & Qin, H. 2016. Higher order volume-preserving schemes for charged particle dynamics. *Journal of Computational Physics*, *305*, 172–184.

16 Fubiani, G., & Boeuf, J. P. 2013. Role of positive ions on the surface production of negative ions in a fusion plasma reactor type negative ion source - Insights from a three dimensional particle-in-cell Monte Carlo collisions model. *Physics of Plasmas*, *20*(11).
17 Fubiani, G., & Boeuf, J. P. 2015. Three-dimensional modeling of a negative ion source with a magnetic filter: Impact of biasing the plasma electrode on the plasma asymmetry. *Plasma Sources Science and Technology*, *24*(5), 55001.
18 Taccogna, F., & Minelli, P. 2017. PIC modeling of negative ion sources for fusion. *New Journal of Physics*, *19*(1).
19 Taccogna, F. 2015. Monte Carlo Collision method for low temperature plasma simulation. *Journal of Plasma Physics*, *81*(1).
20 20. Brieda, L. 2019. Plasma Simulations by Example. In *Plasma Simulations by Example*. CRC Press.
21 Delzanno, G. L., & Camporeale, E. (2013). On particle movers in cylindrical geometry for Particle-In-Cell simulations. *Journal of Computational Physics*, *253*, 259–277.
22 Zenitani, S., & Umeda, T. (2018). On the Boris solver in particle-in-cell simulation. *Physics of Plasmas*, *25*(11).
23 Knapp, C., Kendl, A., Koskela, A., & Ostermann, A. 2015. Splitting methods for time integration of trajectories in combined electric and magnetic fields. *Physical Review E - Statistical, Nonlinear, and Soft Matter Physics*, *92*(6), 1–13.
24 Yu, S., Wu, H., Xu, J., Wang, Y., Gao, J., Wang, Z., Jiang, W., & Zhang, Y. 2023. A generalized external circuit model for electrostatic particle-in-cell simulations. *Computer Physics Communications*, *282*, 108468.
25 Itikawa, Y. 1974. Momentum-transfer cross sections for electron collisions with atoms and molecules. *Atomic Data and Nuclear Data Tables*, *14*(1), 1–10.
26 Yoon, J. S., Song, M. Y., Han, J. M., Hwang, S. H., Chang, W. S., Lee, B., & Itikawa, Y. 2008. Cross sections for electron collisions with hydrogen molecules. *Journal of Physical and Chemical Reference Data*, *37*(2), 913–931.